3.3 Antiproton Source Stochastic Cooling

Cooling the large fluxes coming off the target and into the Debuncher and Accumulator is a difficult project. The performance of both systems is a function of the longitudinal density of the incoming beam. We will describe a model and our approach to calculating the longitudinal density delivered from the Debuncher to the Accumulator.

The design choices for the Accumulator stochastic cooling systems were made under the assumption that the Recycler is the final repository for the antiprotons. Since electron cooling performance improves as density increases while stochastic cooling performance declines, we can make some tradeoffs in the system design that optimize it for the maximum flux through the Accumulator rather than maximizing both flux and the momentum density of the accumulated beam.

We will need to upgrade the longitudinal stochastic cooling systems in the Accumulator. The current 2-4 GHz stacktail cooling system, which moves the injected beam from the deposition orbit to the core, was designed to have a maximum flux of ~35 mA/hour. Changes in the system design will be necessary to handle a flux of 60 mA/hour or greater.   We use a numerical simulation of the Fokker-Planck equation[23], which includes beam feedback, to predict the performance of the upgrade design.

3.3.1 Antiproton Longitudinal Phase Space

3.3.1.1 Introduction

In this section, the longitudinal phase space of the beam during $\overline{p}$ stacking is traced from the beginning of proton bunch rotation at 120 GeV in the Main Injector to the point at which pre-cooled antiprotons are ready for extraction to the Accumulator. The purpose of this examination is to determine what, if any, performance upgrades are required to achieve a sufficiently narrow $\overline{p}$ momentum spread for stochastic momentum stacking in the Accumulator at the required rate. The processes affecting longitudinal phase space during this part of the stacking cycle are: Main Injector bunch rotation, targeting and collection, Debuncher bunch rotation, and Debuncher momentum cooling. The impact of each of these processes on the longitudinal phase space of the beam will be considered in sequence.

The starting point of the calculations that follow is an estimate of the longitudinal emittance (s_p) of the proton beam at 120 GeV in the Main Injector prior to bunch rotation. This estimate is derived from an ESME[24] model of slip stacking at 8.9 GeV/c in the Main Injector[25]. The phase space distribution of two combined Booster batches prior to acceleration in the Main Injector is shown in Figure 3.3.1. The phase space volume occupied by the beam in this figure is not matched to the RF bucket. Consequently, filamentation will cause the beam to fill up the unoccupied phase space within the bucket and the longitudinal emittance of the beam will approach the RF bucket area. Assuming an additional dilution of 10 to 15% during acceleration and transition crossing, the final proton longitudinal emittance at 120 GeV prior to bunch rotation is estimated to be: $s_p = 0.35$ eV-sec.
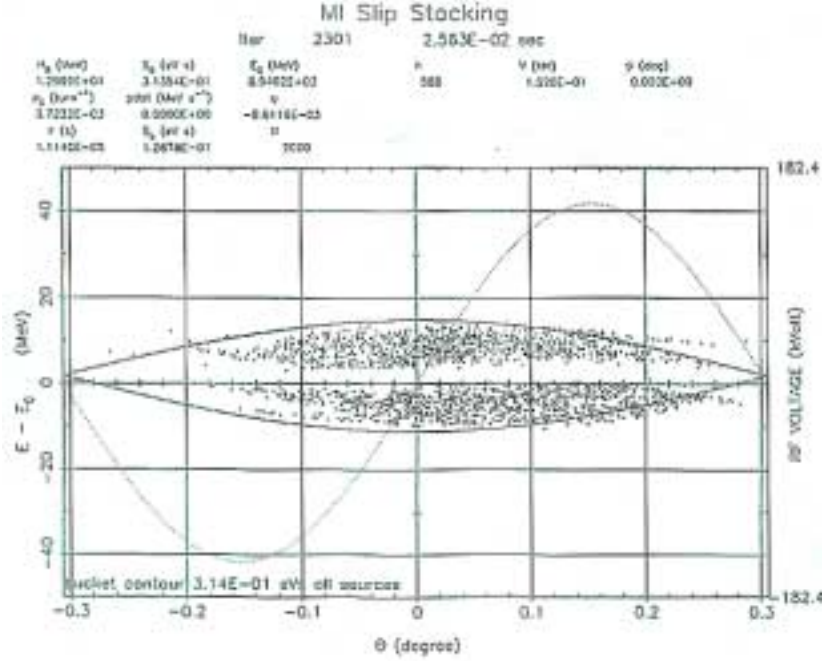
Figure 3.3.1 *Longitudinal phase space distribution of two combined Booster batches at 8.9 GeV/c in the Main Injector. The RF bucket area is 0.31 eV-sec.*

3.3.1.2 Main Injector Bunch Rotation

Main Injector bunch rotation consists to two 90° rotations in longitudinal phase space that function to minimize the bunch length of the proton beam prior to extraction onto the $\bar{p}$ production target. The sequence of RF manipulations that accomplish this is illustrated in Figure 3.3.2. Table 3.3.1 summarizes the Main Injector parameters used in the Run IIb bunch rotation model[i].

Beam Energy	E	120	
GeV Longitudinal Emittance	s_p	0.35	eV-sec
Maximum RF Voltage	V_{max}	4.0	MV
Low voltage value	V_{low}	500	kV
Final Bunch Length (95% Full Width)	**Δt**	**809**	**psec**
Final Energy Spread (95% ½ Width)	**$\Delta E/E$**	**0.185**	**%**

Table 3.3.1 *Main Injector Bunch Rotation Parameters*

The increased proton longitudinal emittance from slip stacking causes a slower rotation velocity for high amplitude protons during the final rotation at high voltage. This has the effect of adding beam to the tails of the final bunch length distribution. Figure 3.3.3 compares the nearly linear rotation of 0.10 eV-sec bunches with that of the

---

[i] The Main Injector bunch rotation model is an ESME model that was originally constructed by Ioanis Kourbanis.

0.35 eV-sec bunches expected during slip stacking. The final slip stacking bunch length and energy distributions are shown in Figure 3.3.4.
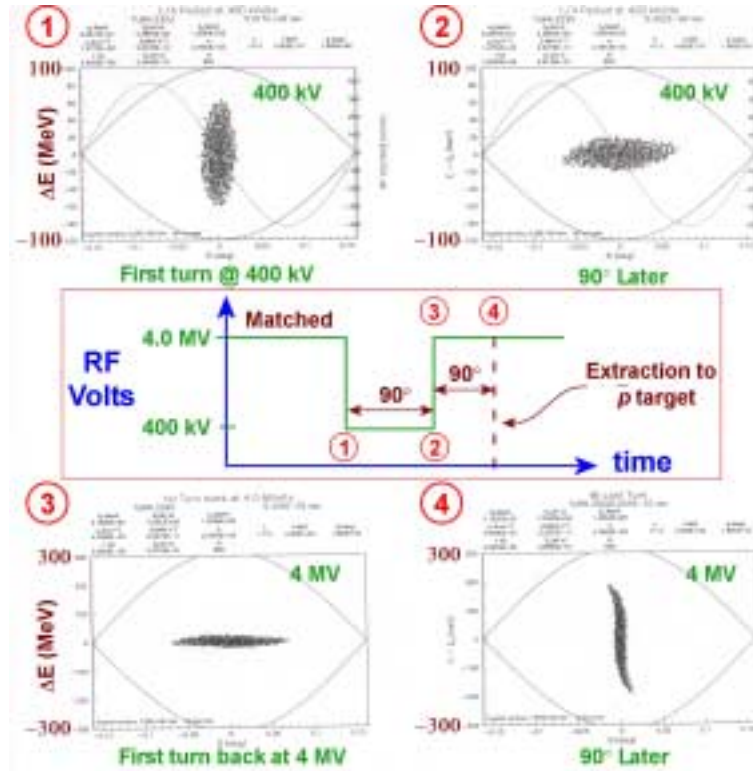

Figure 3.3.2 *The sequence of Main Injector RF manipulations during bunch rotation. The shape of the longitudinal phase space volume occupied by the beam at the various points shown is typical of near linear bunch rotation. Prior to bunch rotation, the phase space occupied by the beam is matched in 4.0 MV buckets. The sequence is initiated by para-phasing the RF cavities down to a few hundred kV (the exact value of the low voltage setting is determined by the longitudinal emittance of the beam). The beam, which is no longer matched to the RF bucket, begins to tumble in phase space (points ① to ②). After a quarter of a synchrotron period, the voltage is rapidly brought back to 4.0 MV (point ③). Since the beam is still unmatched, it will continue to rotate in phase space. The beam is extracted to the $\bar{p}$ production target after another quarter period rotation at 4.0 MV (point ④). At this point, the bunch length of the beam is at its minimum.*

It is interesting to note that the bunch length of protons on the $\bar{p}$ production target expected from the Main Injector during slip stacking is very nearly the same as the bunch length that was realized in Run Ib[i] ($s_p \approx 0.25$ eV-sec) from the Main Ring. This coincidence is entirely accounted for in terms of the difference between the Main Ring and the Main Injector. For linear bunch rotation, the following relationship between Main Injector and Main Ring bunch lengths is true:

---

[i] Run Ib parameters – Longitudinal emittance: $s_p \approx 0.25$ eV-sec, measured bunch length: $\Delta t_{MR} = 800$ psec.

$$\Delta t_{MI} = \sqrt{\frac{s_{MI}}{s_{MR}}} \left(\frac{\eta_{MI}}{\eta_{MR}} \frac{h_{MI}}{h_{MR}} \right)^{\frac{1}{4}} \Delta t_{MR}$$

$$; \quad \sqrt{\frac{0.35}{0.25}} \left(\frac{0.0020}{0.0028} \frac{588}{1113} \right)^{\frac{1}{4}} \Delta t_{MR}$$

$$; \quad (0.774) \sqrt{\frac{0.35}{0.25}} \Delta t_{MR}$$

(3.3.1)

The actual bunch length is slightly larger than that predicted by Eq. (3.3.1) since the rotation for the longitudinal emittance produced by slip stacking is not completely linear.

The large momentum spread of the proton beam after bunch rotation in the Main Injector gives rise to two issues. First, the momentum aperture of the P1, P2, and AP1 beam lines must be large enough to accept the large momentum spread of the proton beam after bunch rotation. This is in fact the case. Secondly, the dispersion function at the target must be small to avoid an increase in the proton spot size with increasing $\Delta p/p$ and the resulting reduction in $\overline{p}$ yield. This also is accomplished in the present AP1 beamline lattice.
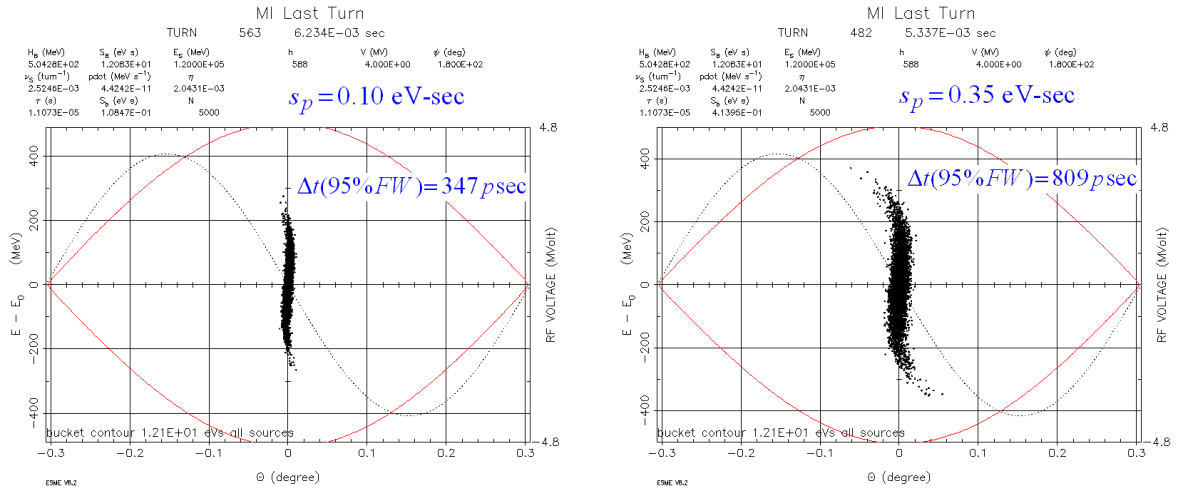

Figure 3.3.3 *Linear and non-linear bunch rotation. Each graph shows the final phase space distribution of the 120 GeV proton beam just prior to extraction. The graph on the left shows the final distribution for protons with an initial longitudinal emittance of 0.1 eV-sec. The graph on the right shows the final distribution for protons with the initial longitudinal emittance expected during slip stacking (0.35 eV-sec). The rotation of high amplitude particles is slower than that of small amplitude particles resulting in tails in the azimuthal distribution.*
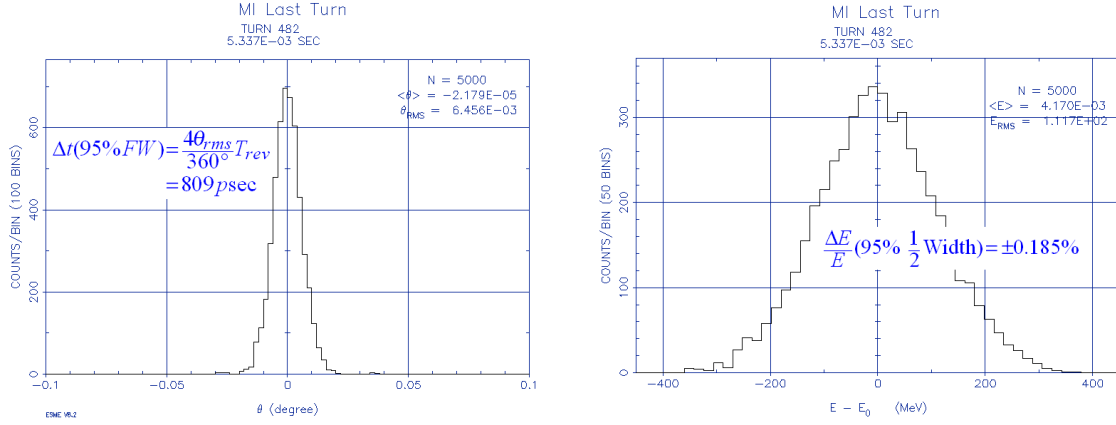
N = 5000
$\langle\theta\rangle = -2.179E-05$
$\theta_{RMS} = 6.456E-03$

$$\Delta t(95\% FW) = \frac{4\theta_{rms}}{360°} T_{rev}$$
$$= 809 \, psec$$

COUNTS/BIN (100 BINS)

θ (degree)

N = 5000
$\langle E\rangle = 4.170E-03$
$E_{RMS} = 1.117E+02$

$$\frac{\Delta E}{E}(95\% \, \tfrac{1}{2}\text{Width}) = \pm 0.185\%$$

COUNTS/BIN (50 BINS)

$E - E_0$ ⟨MeV⟩

Figure 3.3.4 *Final θ (= 2πf$_{rev}$Δt) and ΔE distributions for Main Injector bunch rotation during slip stacking. The θ distribution on the left shows a final proton bunch length of 809 psec (95% full width). The ΔE distribution on the right shows a final ΔE/E of 0.185% (95% half width).*

3.3.1.3 Targeting and Collection

The momentum acceptance of the AP2 beam line and the Debuncher is ±2% (±180 MeV/c at 8.9 GeV/c). The $\overline{p}$ production cross-section is essentially constant over this range of energies. Thus, the energy distribution of antiprotons with energies that fall within the momentum aperture of the AP2 line and Debuncher is uniform in energy. Furthermore, since the time scale of the $\overline{p}$ producing proton-nucleon interactions in the target is negligible in comparison to the bunch length of the incident protons, the time structure of the beam from the Main Injector is preserved.
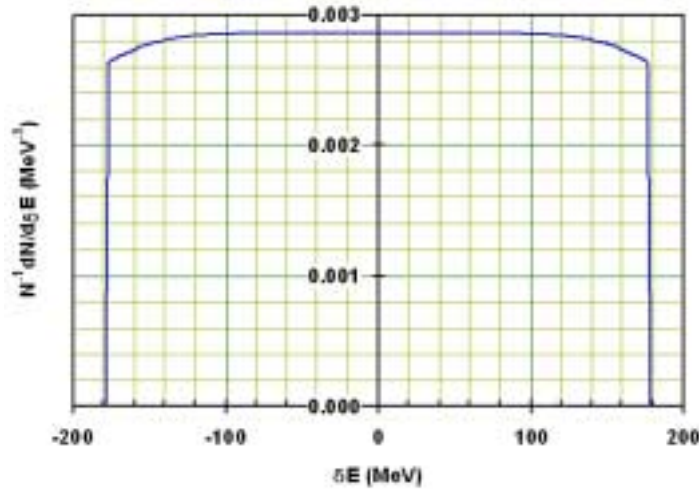
$N^{-1} dN/d\delta E$ (MeV^{-1})

δE (MeV)

Figure 3.3.5 *Calculated energy distribution of the $\overline{p}$ beam collected from the target into a ±2.0% momentum aperture with a central momentum of 8886.3 MeV/c. The transverse emittances are: ε$_x$ = ε$_y$ = 40 π mm-mrad. The momentum aperture limit is assumed to be located at the DRF3 RF cavity in the Debuncher.*

105

The finite transverse emittances of the $\bar{p}$ beam will modify the momentum distribution at the edges of the aperture. Figure 3.3.5 shows the expected $\bar{p}$ energy distribution just after injection into the Debuncher. This distribution is used as the initial energy distribution for the Debuncher bunch rotation calculation.

3.3.1.4 Debuncher Bunch Rotation

A second RF bunch rotation is performed in the Debuncher. This time the rotation converts the narrow time structure of the beam from the target into DC beam with a narrow energy distribution. The sequence of RF manipulations in Debuncher bunch rotation is illustrated in Figure 3.3.6. The parameters that determine the Run IIb Debuncher bunch rotation model are summarized in Table 3.3.2. The expected $\bar{p}$ energy distribution after bunch rotation is shown in Figure 3.3.7.

Beam Energy	E	8935.7	
Slip factor	η	0.00607	
Momentum Acceptance (95% ½ width)	$\Delta p/p$	±2.0	%
Initial Bunch Length (95% full width)	Δt	809	psec
Rotator Cavity Sum Voltage	V_{rot}	5.0	MV
Bunch Rotation Time	t_{rot}	60	msec
Final Energy Spread (95% ½ Width)	$\Delta E/E$	**±0.134**	**%**
Final Energy Spread (95% ½ Width)	ΔE	**±12**	**MeV**

Table 3.3.2 *Debuncher Bunch Rotation Parameters*

The relationship between the proton bunch length and Debuncher $\Delta p/p$ after bunch rotation was calculated for the TeV33 Report[2]. The results of this calculation are shown in Figure 3.3.8. This analysis indicates that very little is gained by reducing the proton bunch length below 800 psec. Furthermore, the minimum $\Delta p/p$ achievable with the present Debuncher RF bunch rotation is approximately 0.25%. The cause of this performance limit is the finite amount of time that is required to drive the rotator cavity voltage down to 90 kV from 5 MV. During this time the beam is still rotating in phase space with the rotation becoming increasingly non-linear as the voltage is lowered. The resulting S-shaped phase space volume will always have a larger energy spread than the flat line that would be obtained if the rotation were linear.

Two remedies to this non-linear rotation in the Debuncher have been considered: (1) second harmonic (106 MHz) correction, and (2) a reduction in the value of η in the Debuncher. Neither of these remedies, when implemented without the other, gives any appreciable improvement in bunch rotation for initial bunch lengths below 1 nsec. If, however, both are implemented together, the model suggests that the reduction of $\Delta p/p$ would continue well below an initial bunch length of 1 nsec (see Figure 3.3.8). Implementation of these bunch rotation improvements is likely to be difficult and costly. Moreover, the improvement indicated for the initial bunch length expected during slip stacking is small. Therefore, they are not presently included in the scope of the upgrades proposed for Run IIb.
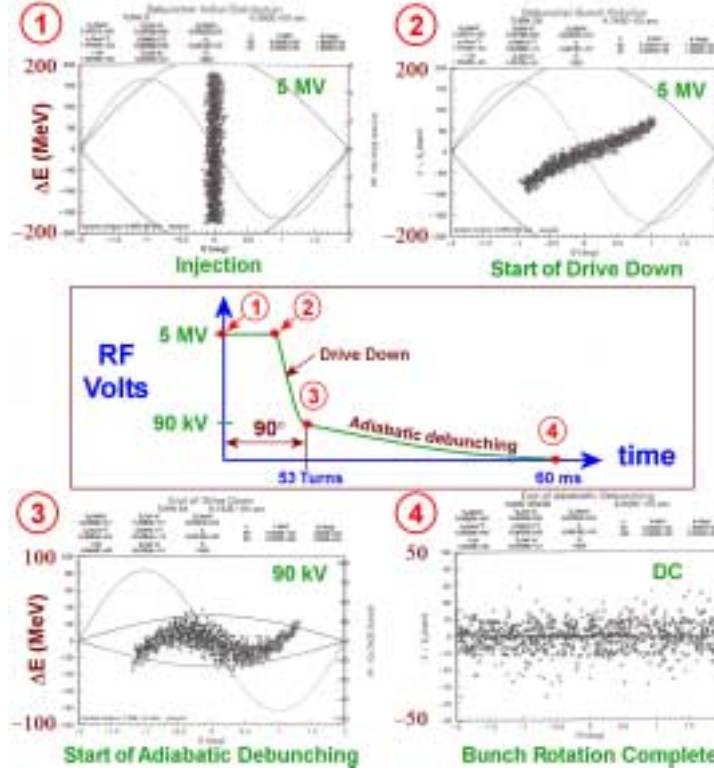
Figure 3.3.6 *The sequence of RF manipulations during bunch rotation in the Debuncher. The $\overline{p}$ beam is injected into the Debuncher into 5.0 MV RF buckets that are synchronized in phase to the Main Injector RF system. The beam, which is not matched to the RF bucket, begins to rotate in phase space (points ① to ②). After a time that is somewhat less than quarter of a synchrotron period, the voltage is rapidly driven down to about 90 kV (point ③). The beam is then adiabatically debunched (point ④).*
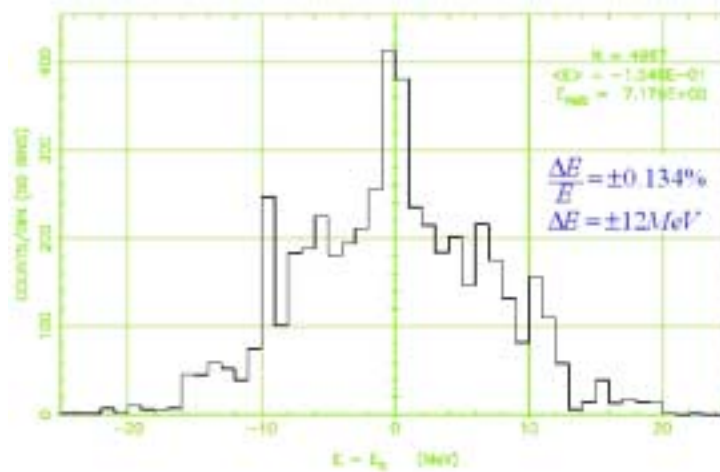

Figure 3.3.7 *ESME model calculation of the $\overline{p}$ energy distribution immediately after bunch rotation in the Debuncher. The widths indicated here are 95% half widths.*
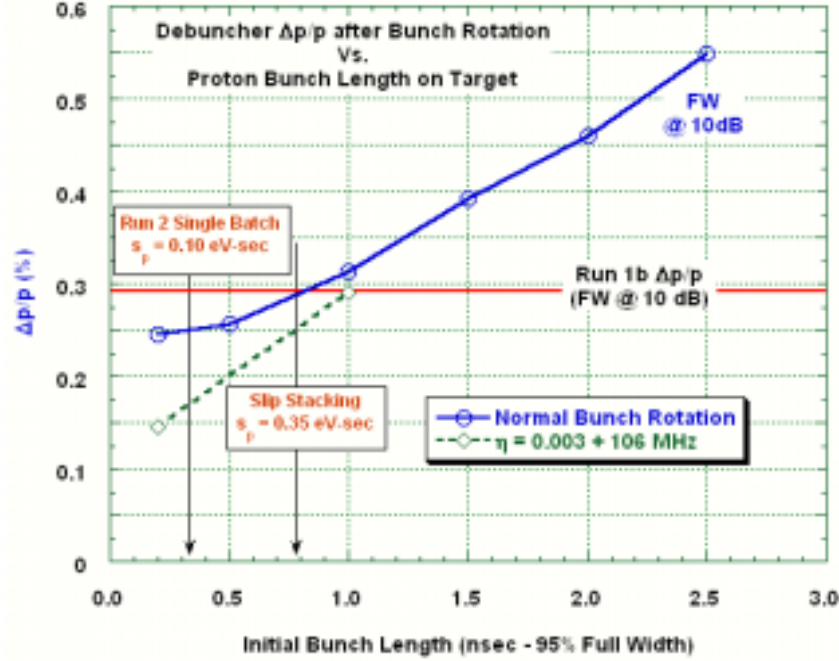
107

Figure 3.3.8 $\bar{p}$ *momentum spread ($\Delta p/p$) versus the bunch length of protons on the $\bar{p}$ production target. The dashed green line is the model prediction of bunch rotation performance if the value of η was reduced by a factor of two and second harmonic correction added to the Debuncher bunch rotation RF system.*

3.3.1.5 Debuncher Momentum Cooling

After bunch rotation, the $\bar{p}$ beam remains in the Debuncher for the remainder of the stacking cycle. The beam is extracted to the Accumulator immediately prior to the arrival of a new batch of antiprotons. The time between bunch rotation and extraction is used to cool the beam in all three dimensions.

Momentum cooling in the Debuncher is accomplished by a recently installed 4-8 GHz filter cooling system. A simple model of Debuncher momentum cooling has been constructed. The model is based on the design parameters of the system rather than on measured quantities[i]. Moreover, this model does not solve the Fokker-Planck equation for the time evolution of the energy distribution of the beam. Rather, the cooling rate of the system is determined by taking the second moment of each term and solving for the time dependence of $\langle E^2 \rangle$.

The model was "tested" by using the parameters of the Debuncher momentum cooling system envisioned in the TeV33 report[2]. The present model gives the same cooling rate and predicts the same thermal and schottky noise power as the model used for the TeV33 study. An upgraded model is being developed, which will be calibrated by measurements of the installed equipment. The present model, however, should be adequate to provide an estimate of the ideal performance of the Debuncher momentum

---

[i] Presently the measurement data available are insufficient to characterize the system.

cooling system.   Table 3.3.3 summarizes the parameters used in the Debuncher momentum cooling model.

Beam Parameters:			
Intensity[i]	N	3.5×10^8	$\dot{p}$ s
Initial Momentum Spread (95% ½ Width)	$\Delta p/p$	±0.134	%
Machine Parameters:			
Cooling time[ii]	Δt	1.94	sec
Revolution frequency	f_{rev}	590035	Hz
η		0.00607	
Cooling Hardware Parameters:			
Pickup and Preamp effective temperature	T_{pu}	35	°K
Number of slotted waveguide pickups[iii]	N_{pu}	16	
Number of slotted waveguide kickers[iv]	N_k	32	
Average pickup impedance	Z_{pu}	12.5	kΩ
Average kicker impedance	Z_k	16.2	kΩ
Electronic gain	g_e	145	dB
Initial Noise Power:			
Thermal noise power		293	W
Schottky noise power		4507	W
Maximum power[v]		4800	W
Cooling time	τ	**0.26**	**sec**

Table 3.3.3 *Debuncher Momentum Cooling Parameters*

The 4-8 GHz bandwidth of the Debuncher momentum cooling is divided up into eight pickup and four kicker bands.[26] The variation of pickup and kicker impedance is shown in Figure 3.3.9 and Figure 3.3.10. The momentum cooling model uses an inverted parabola approximation to represent the variation of pickup and kicker impedance with frequency in each microwave band.

The electronic gain of the system includes a notch filter response. The model implements this as an ideal notch filter with a transfer function given by:

$$G_{fil}(f) = \frac{i}{2}\left(1 - e^{-2\pi i f T_{rev}}\right)$$

(3.3.2)

where T_{rev} is the central orbit revolution period. The notch filter provides the energy discrimination required for the coherent part of the signal while simultaneously rejecting the noise signals at frequencies near harmonics of the revolution frequency.

---

[i] This is based on a stacking rate of 60 mA/hr.
[ii] This number is the stacking cycle time (2.0 sec) minus the time required for Debuncher bunch rotation (60 msec).
[iii] 8 bands in both planes.
[iv] 4 bands in both planes.
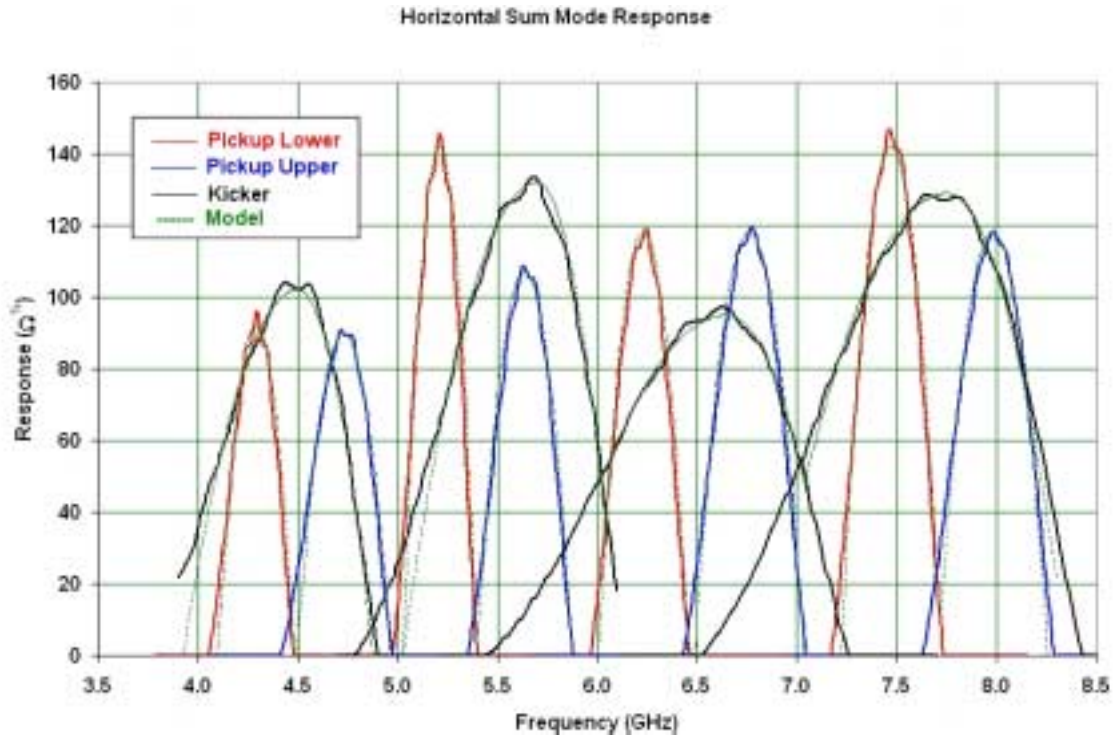[v] The power limit is determined by a 150 W limitation for each TWT. There are 32 TWTs in the system.

Figure 3.3.9 *Horizontal pickup and kicker impedances. The variation of the impedance for each band is represented by an inverted parabola in the momentum cooling model. The modeled Z(f) is shown by the dashed green line.*
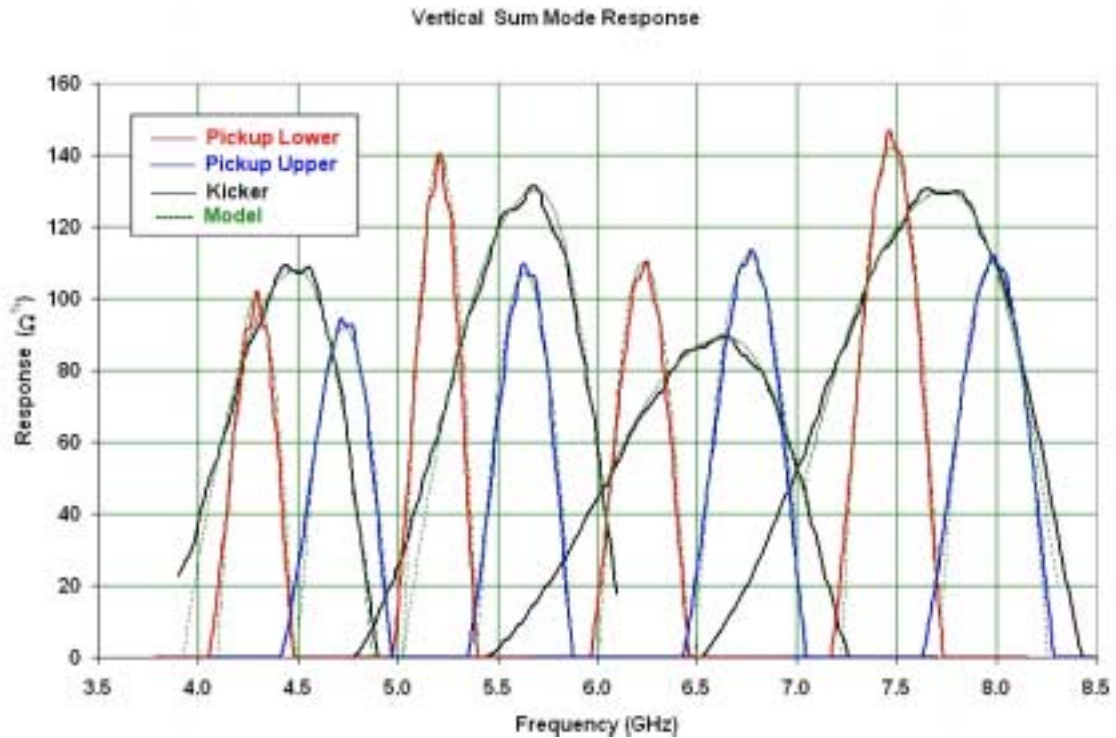

Figure 3.3.10 *Vertical pickup and kicker impedances. The variation of the impedance for each band is represented by an inverted parabola in the momentum cooling model. The modeled Z(f) is shown by the dashed green line.*

The overall system gain of the system, g_e, is limited by the maximum allowed power output to the kickers. The power output is primarily due to pickup and amplification of the schottky noise of the beam. In this regime, the maximum allowed gain decreases approximately as the inverse square root of the beam intensity[i]. Accordingly, the contribution of pickup and amplifier noise to the total noise power decreases with increasing beam intensity.

The present Debuncher momentum cooling model predicts a cooling time of 0.26 sec under Run IIb stacking conditions. This cooling time is at least a factor of five better than what has been observed with the system to date. While it is likely that the predicted cooling time will be adjusted upward as the model is refined; it is also likely that substantial increases in the performance of the installed hardware will be realized as the system is tuned-up. It seems reasonable to assume therefore, that Debuncher momentum cooling will accomplish the reduction in momentum spread required for stochastic stacking in the Accumulator.

3.3.2 Description of stochastic stacking

Stochastic stacking with a constant flux is achieved by designing a system with gain as a function of energy that falls exponentially, with characteristic energy E_d. The resulting density distribution then rises exponentially with the same characteristic energy[27]. The resulting maximum flux Φ can be expressed as:

$$\Phi = \frac{W^2 \eta E_d}{f_0 p \ln(F_{\min}/F_{\max})}$$

(3.3.3)

where W is the bandwidth of the system, η is the phase slip factor, f_0 is the beam revolution frequency, p is the beam momentum, and F_{min} and F_{max} are the minimum and maximum frequencies in the system bandwidth. Planar pickups have a response which goes like $exp(-\pi x/d)$, where x is the transverse distance from the center of the pickup and d is the vertical aperture. If the pickups are located in a region of high momentum dispersion, we can design a system where the gain response falls off exponentially with energy. The region of exponential density increase is called the 'stacktail' and the region where beam accumulates is called the 'core'. Since the revolution frequency changes with energy and hence the flight time between pickup and kicker is a function of energy but the delay time through the electronics is a constant, it is necessary to use multiple sets of pickups with different gains and delays to build the gain slope across the aperture. Correlator notch filters are used to null out the signal at the core.

The present Accumulator provides a good example of the basic principles. Figure 3.3.11 shows the antiproton density distribution as a function of beam revolution frequency overlaid in the stacktail region with an exponential fit. The maximum flux for

---

[i] The noise power is primarily due to the schottky noise of the beam, which is in turn proportional to the square of the rms beam current: $4800W = P \propto i_{rms}^2 g_e^2 \propto N g_e^2$.

this particular stack is calculated from the results of the fit. Figure 3.3.12 shows the maximum flux from these fits versus stack size for two different stacking periods (in July and Oct 2000). Note that the fitted maximum flux, based on the slope, is of order 30 mA/hour even though the stack rate was about 10% of that number.
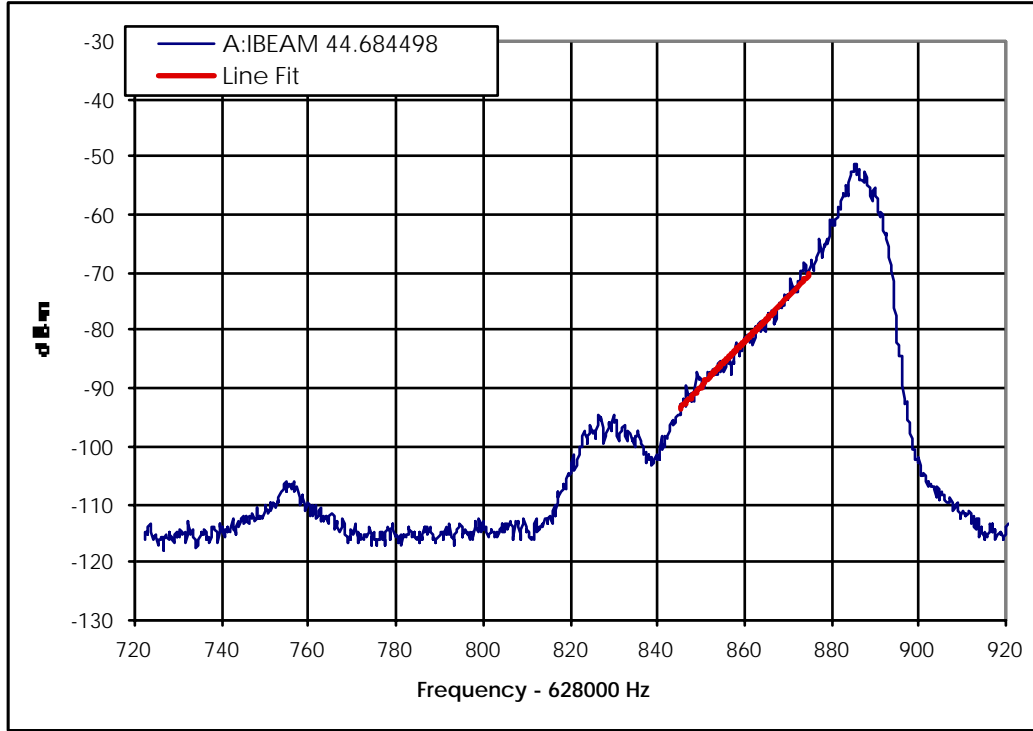

Figure 3.3.11 *Stacking density distribution overlaid with exponential fit in the stacktail region.*

Of the parameters appearing in Eq. (3.3.3) E_d, W, and η are the only ones that can reasonably be considered as changeable. The simplest approach to maximize the flux is to increase E_d. This approach sacrifices the amount of density compaction achievable, since the density grows as $exp(E/E_d)$, but has fewer implications for other systems in the Accumulator. Increasing the bandwidth clearly increases the maximum flux. However, changing the system bandwidth also requires changing the Accumulator lattice parameter η to avoid Schottky band overlap at high frequencies. The design shape of the voltage gain depends on the one-to-one map between position and momentum due to dispersion at the pickups and the corresponding many-to-one map between frequency and momentum. The Accumulator stacktail cooling creates an approximately 100 MeV/c wide "stacktail" in the longitudinal distribution of the stack in order to accommodate the incoming $\bar{p}$ flux. For the present value of η, the longitudinal Schottky bands of the 100 MeV wide stacktail distribution begin to overlap at frequencies above ~4.3 GHz. Therefore, changing the system bandwidth in a way that precludes Schottky band overlap requires changes in the Accumulator lattice.

Changing the system bandwidth was the approach taken in the upgrade that was installed between Collider Run I and Run II. The system bandwidth was doubled (from 1-2 GHz to 2-4 GHz) and η was halved (from 0.023 to 0.013) while maintaining the same E_d. This upgrade is ultimately expected to double the maximum flux. There have been

some drawbacks to this approach. The change in η has impacted the performance of the core stochastic cooling systems due to the concomitant factor of two increase in the mixing factor. Moreover, the change in γ_t that was required to lower η changed the circumference of the Accumulator injection orbit so that the harmonic relationship between it and the circumferences of the other accelerators in the Fermilab complex is now only approximate. Consequently, additional RF manipulations are now required to handle the transfers of antiprotons from the Accumulator to the Main Injector and Recycler. Given these difficulties, a further reduction in η to accommodate another bandwidth increase is very hard to justify.
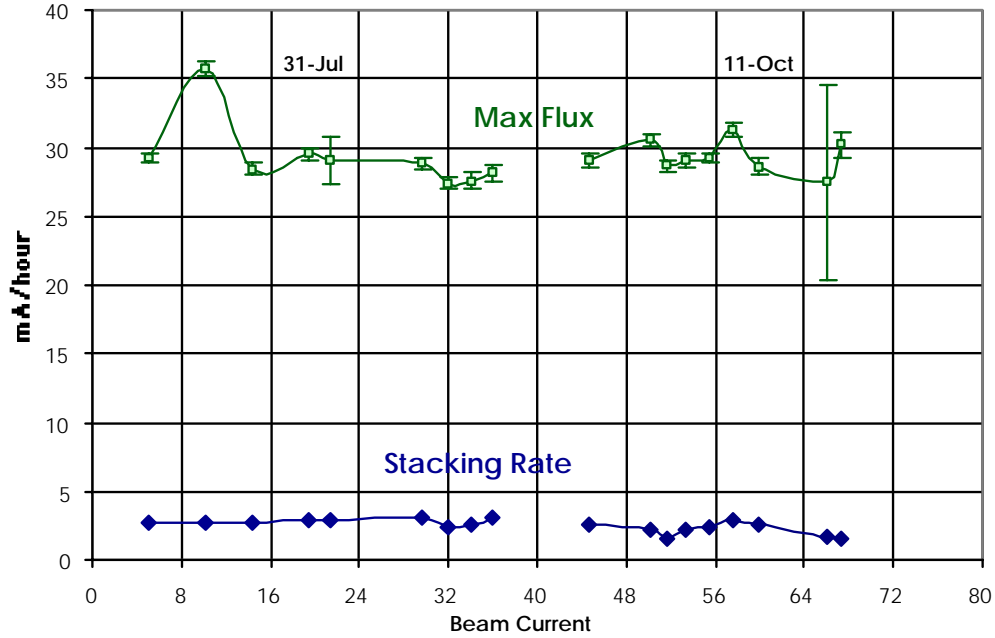

Figure 3.3.12 *Flux results (mA/hour) vs. stack size*

There are also drawbacks to the approach proposed here – increasing E_d. The Accumulator has a finite momentum aperture. It is therefore necessary to stop the flux at some point and accumulate it. In so doing, the gain function deviates from the pure exponential and other considerations come to the fore. It is necessary to match the stacktail system gain to the core system gain to have a smooth transition in the gain profile. As the density increases, diffusive beam heating from other particles (through the cooling systems) eventually dominates the cooling term and the system is no longer able to effectively increase the density. It is generally true that as the density of the core increases it becomes necessary to decrease the system gain to maintain some margin between the cooling and diffusive terms of the Fokker-Planck equation.

Another limitation is the assumption of constant input flux. The input flux is a transient, with large pulses of beam coming every 2 seconds. It is necessary for the input pulse to move completely into the stacktail region before the next pulse arrives. Any beam that remains will be phase displaced by the RF bucket moving the new pulse onto the deposition orbit. The fraction of the input pulse that moves across the aperture is a function of the gain of the system and the momentum distribution of the input pulse. The larger the gain, the more efficiently the input pulse moves off the deposition orbit. The

large gain necessary for the effective stacking of the input pulse is also detrimental, for the reasons given above) to accumulating large amounts of beam in the core. With some simplifying assumptions[28], the fraction of the beam that moves off the deposition orbit as a function of the time between input pulses can be calculated. Figure 3.3.13 shows this calculated fraction for a system that is representative of the Run IIb design. Note that for a 2 second cycle time the system fails to move 100% of the beam off the deposition orbit (the 100% mark is reached at 2.5 seconds). Increasing the gain by 3 dB moves the 100% mark down to 1.8 seconds.
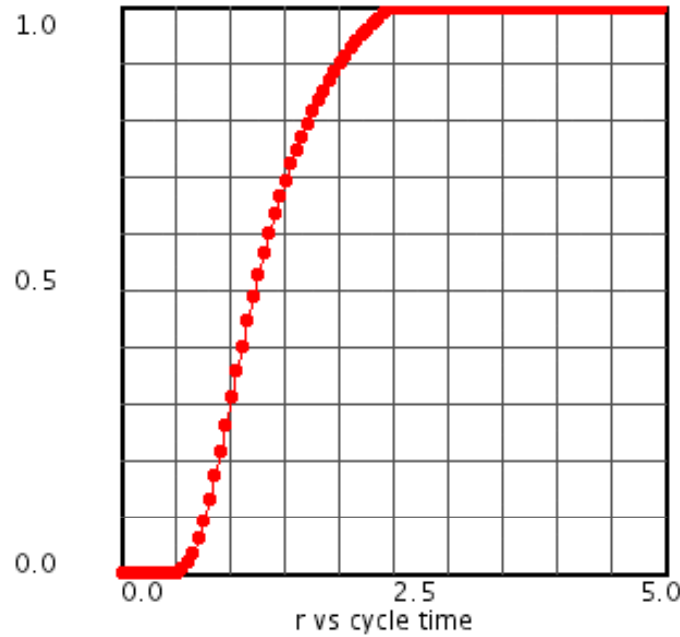
Figure 3.3.13 *Fraction of beam that moves into the stacktail region as a function of cycle time. This model is for 80 mA/hour injected and reasonable selections of the gain.*

3.3.3 System parameters

The system is being designed with the goals of handling an input flux of 80 mA/hour, a 2 second cycle time, an injection bucket height of 6 MeV at h=84, efficiencies greater than 95% for 30 minutes of stacking time, using a bandwidth of 2-4 GHz in the stacktail and 4-8 GHz in the core. To reach this goal a gain slope of 18 MeV is required. This gain slope can be achieved and the above design goals met with modifications to the current stacktail system (described below). The modifications include changing the central energy of the pickup tanks (by moving the tanks several millimeters) and adjusting the electronics gain and phase settings.

Figure 3.3.14 shows an example calculation of the gain as a function of energy. With 2 pickups, an 18 MeV gain slope can be designed. The required gain for the core system is large; therefore, as the density grows, it becomes necessary to lower the gain.

Figure 3.3.15 shows 30 minutes of stacking with the system gain from the previous figure. Several adjustments to the gain were made during the simulation because of the diffusive heating problems. An average stacking rate of 75.34 mA/hour was achieved.
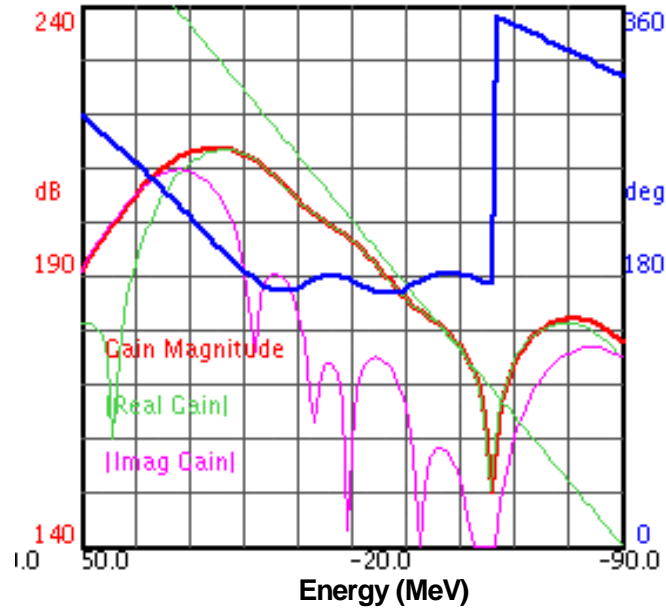
Figure 3.3.14 *Example gain slope calculation for two pickups in the stacktail and a 2-4 GHz core cooling system. Red is the magnitude, green is the real part (which does the cooling), purple is the imaginary part (which heats the beam), and blue is the overall system phase. The straight green line is a gain slope of 10 MeV for comparison.*
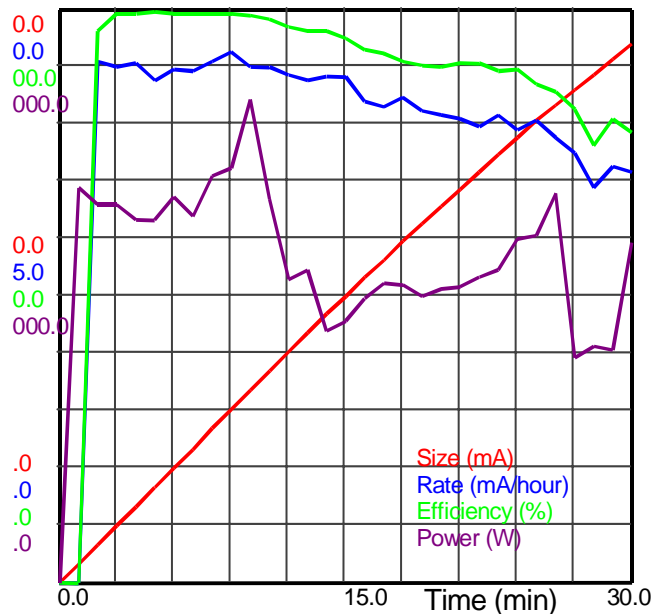

Figure 3.3.15 *Stack size, rate, efficiency, and power for 30 minutes of stacking with above configuration. The large changes in power occur when the gain is turned down because of diffusive heating problems. After 30 minutes, 37.67 mA are accumulated.*

The stacktail system consists of two sets of pickups (see Figure 3.3.16 for schematic), with independent gain and delay control. The pickups are kept at liquid nitrogen temperature to minimize electronic noise. There are 128 pickup loops at 15

115

MeV (with respect to the central energy of the Accumulator) and 48 pickup loops at -8 MeV. There are 128 kicker loops in 8 tanks, with 4 TWTs per tank. There is approximately 150 dB of gain from pickup to kicker. The system also makes provision for combining the signals from the 2 sets of pickup loops (and a 3rd set, not included in the figure) to fine tune the gain shape (called "compensation legs").
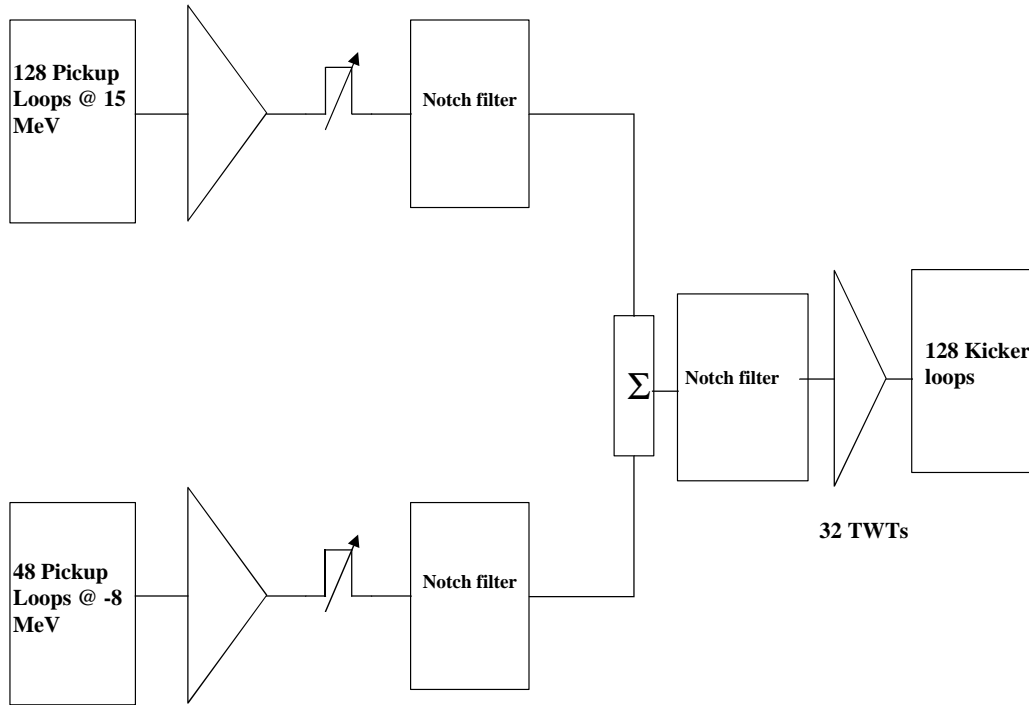

Figure 3.3.16 *Schematic diagram of the Run IIb stacktail cooling system. There are two sets of pickups at different energies, with independent gain and delay control. The system electronics has a total gain of 150 dB.*

3.3.4 Performance of the current system

The current stacktail system is functionally identical to that described above, with the exception of the pickup positions (energies) and the relative gain and delay settings. Currently, there are 128 pickup loops at 16 MeV (with respect to the central energy of the Accumulator), 48 pickup loops at the central energy, and an additional 16 pickups at -23 MeV (as a compensation leg). The pickups are kept at liquid nitrogen temperature, with a calculated effective system noise temperature of 125 K.

The current maximum stacking rate that has been achieved to date is 10 mA/hour with a 2-second cycle time, while the maximum flux (based on exponential slope) approaches 30 mA/hour. Detailed simulations of the current stacktail system have been performed. The simulated peak performance agrees well with the 30 mA/hour maximum flux from beam measurements. Figure 3.3.17 shows the simulated performance. The input flux in the simulation was adjusted until the maximum efficient stacking rate with a

2-second cycle time was achieved. After a short time period, the system reached a stable stacking rate of ~37 mA/hour. Fits to the density profile similar to those discussed in section 3.3.2 correspond to a flux of 38 mA/hour.
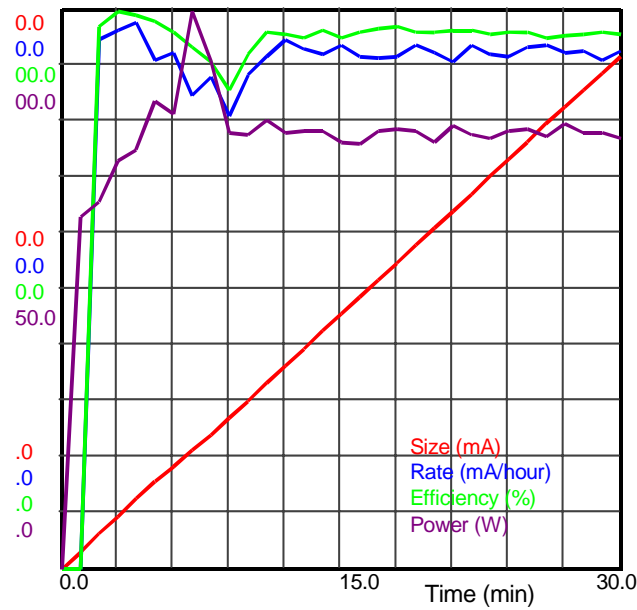

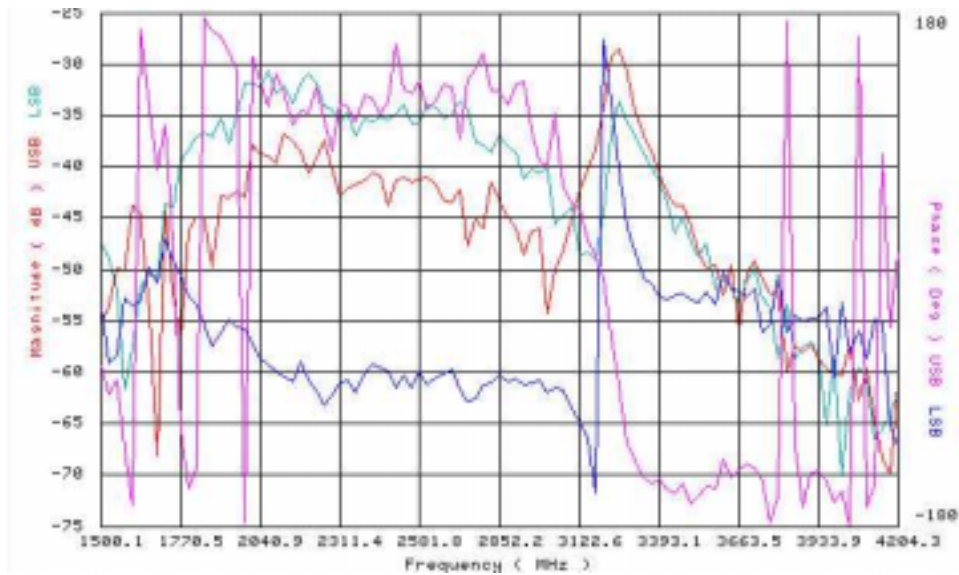Figure 3.3.17 *Simulated performance of current Run II stacktail cooling system.*

Figure 3.3.18 *Response on the Core Horizontal βtron pickup to excitation by the stacktail kickers. Note the large response near 3.2 GHz (blue is the upper sideband, red is the lower sideband).*

Presently the stacking rate is limited by the input flux into the Accumulator. This is partly because stacking cycle times shorter than 2 sec have not been utilized. There have been two problems identified with running high power in the current stacktail cooling system.

117

The first problem involves a correction system, known as the 'delta kickers'. The delta kickers are a set of 4 TWTs connected to the stacktail kicker tanks in delta mode, phased to null out any transverse kicks from imperfections in the mechanical construction or alignment of the stacktail kicker tanks. Figure 3.3.18 shows the response of the core horizontal betatron pickup when the stacktail kickers are excited. There is a large response near 3.2 GHz, which has been associated with a difference mode launched in the kicker tank. The magnitude of this response is too large for the delta kickers to compensate for, as they do not have a similar spike in response around 3.2 GHz (see Figure 3.3.19). As a result, operation of the stacktail at high power causes transverse heating of the core.
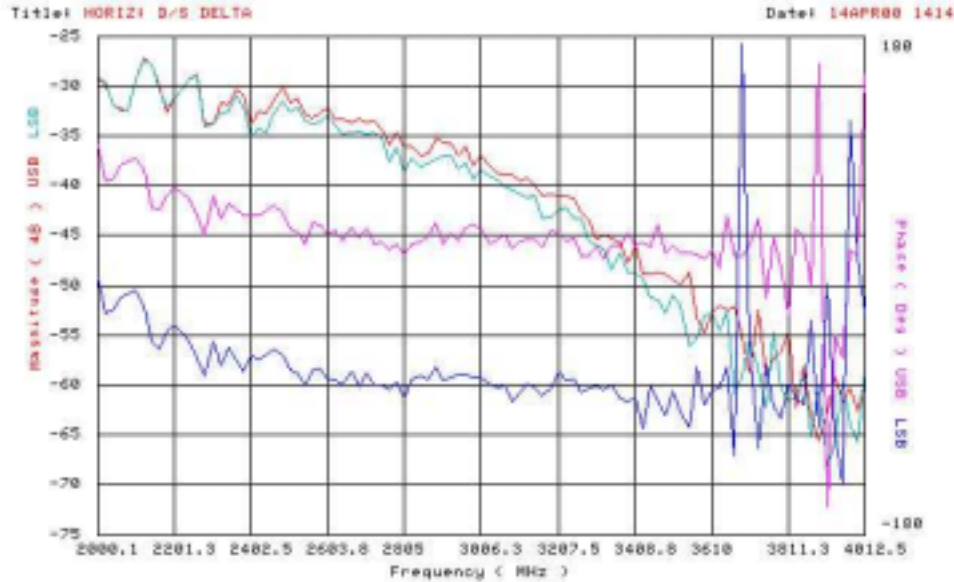

Figure 3.3.19 *Delta kicker response versus frequency*.

The second limitation to the power in the stacktail is that the system goes unstable at high power and large stacks. This instability occurs because the high density beam at the core responds coherently to the stacktail kicks, oscillating at the frequency where the kick is the largest and the gain the highest. Since the stacktail compensation legs, designed to null out the pickup response of near the core, have not yet been phased in properly, this signal shows up on the stacktail pickups. Eventually, the system goes into positive feedback mode somewhere in the 2-4 GHz frequency band. The compensation legs will be commissioned in the near term future.

3.3.5 Project Plan

Since the design for Run IIb stacktail cooling requires only moving the stacktail pickup tanks a few millimeters from their present position, with the additional changes to gain slope accomplished by adjusting relative gain and delay of the electronics, the plan is simple to implement. The pickup position changes could be done during a one-day shutdown of the Accumulator. Some additional beam study time will be required to measure and adjust the system settings. From the point of view of resource availability,

the stacktail upgrade is ready to go now. However, since the present operation of the Accumulator requires the accumulation of large stacks, implementation of the stacktail upgrade should be delayed until larger fluxes are available. Operation of the upgraded stacktail system would seriously compromise the performance of the Accumulator core cooling systems with large stacks ($\geq$40 mA).

	Total	M&S	Labor	Phys.	Eng.	Draft	Tech	CP
FY02	100	0	100	0.8	0.2	0	0	0
FY03	400	100	300	1	1	0	1	0
FY04	0	0	0	0	0	0	0	0
FY05	0	0	0	0	0	0	0	0
Project	500	100	400	1.8	1.2	0	1	0

Table 3.3.4 *Funding profile for Stacktail upgrade*